

# Reuse and Recycling of Clayey Soil in Pasir Panjang Terminal Phases 3 and 4 Project in Singapore

Loh Chee Kit<sup>1</sup>, Eugene Khoo<sup>2</sup>, Seah Kim Huah<sup>3</sup>, James Lam Pei Wei<sup>4</sup>, Thiam Soon Tan<sup>5</sup>,  
Fumitaka Tsurumi<sup>6</sup> and Takahiro Kumagai<sup>7</sup>

<sup>1</sup>Project Director (Retired), Maritime and Port Authority of Singapore, Singapore

<sup>2</sup>Maritime and Port Authority of Singapore, Singapore

<sup>3</sup>Surbana Jurong Consultants Pte. Ltd., Singapore

<sup>4</sup>Surbana Jurong Consultants Pte. Ltd., Singapore

<sup>5</sup>Singapore Institute of Technology, Singapore

<sup>6</sup>Penta-Ocean Construction Co., Ltd., Tokyo, Japan

<sup>7</sup>Penta-Ocean Construction Co., Ltd., Tokyo, Japan

E-mail: Takahiro.Kumagai@mail.penta-ocean.co.jp

**ABSTRACT:** In order to increase the handling capacity of ports in Singapore, the Maritime and Port Authority of Singapore (MPA) has embarked on massive port development projects for the past decade. One of the major projects was the Reclamation for Pasir Panjang Terminal Phases 3 and 4, completed in April 2015. The project provided 200 hectares of port land equipped with 5.7 km of berthing facilities to accommodate ultra-large container ships. In this project, MPA embraced sustainable development by reusing dredged and excavated clayey soil as reclamation fill and as fill material to form a containment bund within the footprint of the project. Nearly half of the reclamation fill consisted of clayey soil, which was improved using prefabricated vertical drains with surcharge. The containment bund, which served as a temporary earth-retaining system during reclamation filling, was formed using geotextile tubes filled with clayey soil treated with cement. This paper describes the innovative design and construction in the project.

**KEYWORDS:** Container Port, Reclamation, Dredged Material, Cement Mixed Soil, CMS, Containment Bund, Geotextile Tube

## 1. INTRODUCTION

The Port of Singapore is the world's largest transshipment hub. In Singapore, the port has an important role in national development. The Maritime and Port Authority of Singapore (MPA) has carried out major port development projects to increase container handling capacity to meet future growth in seaborne trade.

The expansion of Pasir Panjang Terminal (PPT) by constructing Phases 3 and 4 was planned in 2004 in the southern part of the Singapore shown in Figure 1, not only to increase Singapore's overall container handling capacity by 50%, from 35 to 50 million TEU (Twenty-foot Equivalent Units, meaning a standard-sized shipping container), but also to meet the demand from increasing size of container ships such as ultra-large container ships. With the expansion of PPT, 15 new berths with nearly 6,000m of quay length and 18m draught were added. The expansion of PPT Phases 3 and 4 included land formation of approximately 200 hectares of land. A large volume of filling material of about 50 million cubic meters was required.

Faced with a shortage of good sandy material in Singapore, MPA embraced sustainable development by reusing and recycling clayey soils, such as marine clay and Jurong Formation soil from dredging of fairways and basins and excavated soil from onshore construction projects, for reclamation fill and fill material for a containment bund. The bund, constructed using geotextile tubes filled up with clayey soil treated with cement, served as a temporary earth-retaining system.

The total volume of reclamation fill was approximately 50 million cubic meters, and about 20 million cubic meters of this total volume consisted of clayey dredged and excavated soil. Prefabricated vertical drains (PVD) with surcharge were adopted to improve shear strength and accelerate consolidation of the dredged material used as reclamation fill. Cement-Mixed Soil (CMS) was made from dredged soil and partly filled into the geotextile tubes to form the containment bunds (Geo-Bund). The detailed technical description and applications of CMS is described by Kitazume (2017).

This paper describes innovative geotechnical design and

construction in reusing soft clayey soil as alternative fill materials. By use of these innovative methods, more sustainable development was achieved through reduction of dependence on sand and minimization of the need for disposal grounds for unwanted dredged and excavated material.

## 2. GROUND CONDITIONS AT THE SITE

### 2.1 General geology

The construction site was located in the geological formations of the so-called Kallang Formation and Jurong Formation. Figures 2 and 3 show the schematic geological profiles of coastal deposit of Kallang Formation and stiff Jurong Formation (Singapore Public Works Department, 1976).

The Kallang Formation was formed by recent deposits of soft clays, organic soil, loose sand, etc. usually overlying the Jurong Formation.

Some deep valleys were formed by erosion, in the Holocene period (eleven thousand years ago to present). At the project site, the Kallang Formation is generally composed of marine clay (M), fluvial sand (F1) and fluvial clay (F2).

The Jurong Formation was formed in the late Triassic to early Jurassic (about 100 to 200 million years ago). It is composed of sedimentary rocks such as sandstone, mudstone and limestone, and is characterized by high shear strength and bearing capacity.



Figure 1 Location of the PPT Phases 3 and 4 project in Singapore

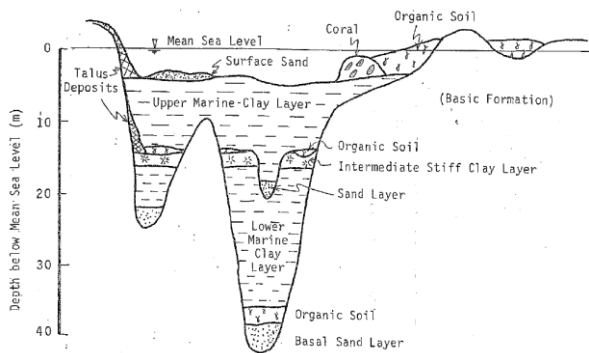


Figure 2 Schematic profile of coastal deposits in Singapore

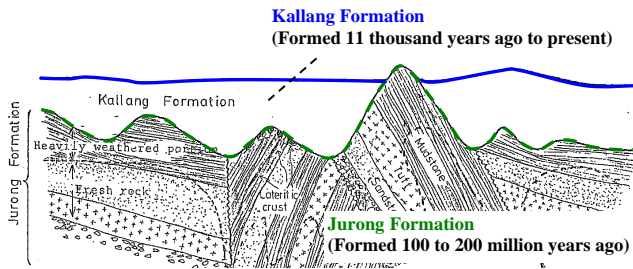


Figure 3 Schematic diagram of structure of Jurong Formation

Based on the logs of numerous boreholes carried out for the project, a typical soil profile at the site is shown in **Figure 4**. In this figure and elsewhere in this paper, negative values in “m CD” are the depths in meters below the chart datum level established by the MPA Hydrographic Department, and positive values are elevations above the chart datum level.

The subsoil conditions are classified as

- (a) Kallang Formation, consisting of M, F1, F2, and very soft surface sediment
- (b) Jurong Formation, categorized based on SPT N-value
  - Residual soil (RS): SPT N-value < 30
  - Residual soil (RS): 30 < SPT N-value < 50
  - Residual soil (RS): 50 < SPT N-value < 100
  - Residual soil (RS): 100 < SPT N-value
- (c) Rock.

Soil samples of the marine clay and residual soil are shown in Photo 1.

### 2.2 Soil properties

A series of physical soil tests was conducted on about 200 soil samples to obtain natural water content, wet density, Atterberg limits, etc.

Table 1 summarizes the mean values of test results for Kallang and Jurong Formations. The marine clay was classified as inorganic clay with high plasticity (CH), and its natural water content was almost twice as high as the other soils. An interesting finding is that the fluvial clay and residual soils have similar mean values of physical properties although their histories of soil formation are quite different. Both are classified as inorganic clay with medium plasticity.

More than one hundred undisturbed soil samples were tested to obtain compressibility parameters. The proposed consolidation parameters used in the design are summarized in Table 2.

### 3 OVERVIEW OF THE CONSTRUCTION SCHEME

Figure 5 shows a conceptual view of construction of Pasir Panjang Terminal Phases 3. The main reclamation area was nearly 1,750 m in the cross-shore direction and 900 m in the long-shore direction. The selected design solution for the wharf structure along the reclamation perimeter was caisson quay walls.

Phase 4 of the project, not visible in the schematic, was a narrower strip of reclaimed land, also with caisson quay wall, along the shoreline linking to the existing Pasir Panjang Terminal (Phases 1 and 2).

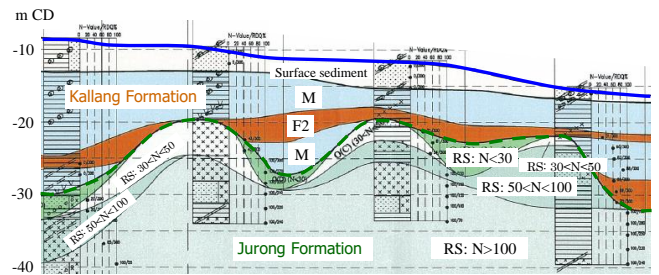


Figure 4 Typical soil profile at the site



(1) Marine Clay (2) Residual soil

Photo 1 Soil samples of the Marine Clay and Residual soils

Table 1 Average physical properties of the soils

(1) Kallang Formation				
Soil type	Marine clay	Fluvial clay		
Natural water content (%)	63	30		
Wet density (Mg/m <sup>3</sup> )	1.64	1.94		
Consistency	Liquid limit (%)	85	52	
	Plastic limit (%)	35	24	
	Plasticity index	50	28	
(2) Jurong Formation				
Soil type	RS (N<4)	RS (N<30)	RS (N<50)	
Natural water content (%)	32	32	25	
Wet density (Mg/m <sup>3</sup> )	1.94	1.93	2.00	
Consistency	Liquid limit (%)	51	51	45
	Plastic limit (%)	25	27	25
	Plasticity index	26	24	21

The containment bunds were constructed as earth-retaining structures to form temporary reclamation edges. The first, shorter bund, bounded the building platform and dock for caisson fabrication and launching. The second bund divided the Phase 3 area in half in the cross-shore direction. This bund had another function, which was to prevent turbidity caused by dredging and filling from spreading to the surrounding natural environment.

In this project, approximately 50 million m<sup>3</sup> of reclamation materials was required while available good sandy soil was only 30 million m<sup>3</sup>. In order to compensate for the acute shortage of good fill materials, methods of reusing and recycling methods on clayey soil were introduced to provide alternative fill material. About 20 million m<sup>3</sup> of clayey soils consisting of the marine clay and residual was derived from fairway and basin dredging works. Some additional clayey soil was supplied from land construction and excavation works.

Figure 6 shows a schematic profile between the caisson quay wall and the containment bund. The dredged clayey soil was mainly placed between the quay wall and the bund. In maximizing the use of dredged clay, the placement of the soil had to be away from the quay wall such that it would not pose a stability problem such as global slip failure.

Table 2 Proposed consolidation parameters used in design

(1) Kallang Formation			
Soil type	Marine clay	Fluvial clay	
Natural void ratio	1.67	0.81	
Compression index	1.06	0.27	
Preconsolidation pressure (kPa)	180	340	
Coefficient of consolidation $c_v$ (m <sup>2</sup> /year)	2	12	
(2) Jurong Formation			
Soil type	RS (N < 4)	RS (N < 30)	
Natural void ratio	0.86	0.87	
Compression index	0.35	0.32	
Over-consolidation ratio	3	5	
Coefficient of consolidation $c_v$ (m <sup>2</sup> /year)	10	15	

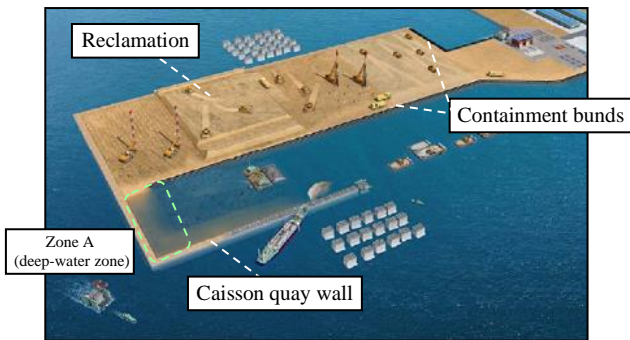


Figure 5 Conceptual view of construction in the project

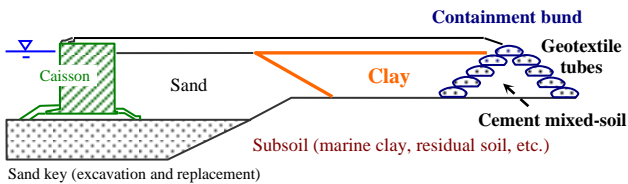


Figure 6 Schematic profile section between the caisson quay wall and containment bund

Since this area was intended to be used as a container yard in the future, the residual settlement during 50 years after completion of the construction was specified to be within 300 mm. To comply with the port requirement, the soft clay fill was improved by accelerating its consolidation with prefabricated vertical drains and surcharging.

The sides of the containment bund were constructed with geotextile tubes filled with clayey soil treated with cement, known as cement-mixed soil (CMS). The CMS was in slurry form at the mixing and filling stages; the geotextile tubes were filled with the treated slurry. The CMS slurry was also cast underwater to form the core body of the containment bund, retained between the geotextile tubes. The filling speed of CMS had to be controlled considering strength development with time. Further explanation is provided in Section 5.

**4 REUSE OF CLAYEY SOIL AS RECLAMATION FILL**

**4.1 Methodology of reusing clayey material as fill**

For filling clayey soils such as dredged clay and excavated clay, the direct dumping method was applied by use of split hopper barges together with pusher boats as shown in Figure 7. After soil was loaded into the hopper of a barge and transported to the

dumping zone, the barge’s split hopper was opened to discharge the soil. Photo 2 shows a hopper barge and soil-dumping operation by opening the barge’s split hopper.

After the level of dumped soil reached the draft limit of the hopper barges, the shallow area was reclaimed up to the planned level of -1.0 m CD by fill brought in on flat-top barges equipped with excavators.

Following the filling of clayey soil, a 1-m thick sand layer, called a sand mat, was placed on the clay layer. This sand mat provided a bearing layer to prevent localized slip failure or mud flow during subsequent sand filling to form a working platform at +3.5 m CD. PVD was installed from this working platform.

Photo 3 shows the reclamation of sand fill and PVD installation.

For accelerating consolidation of clayey fill and original soft clay layer, surcharge fill was placed. The design load of surcharge at the level of +4.5 m CD was set at 180 kPa considering the future load of 155 kPa with the pavement load of 12 kPa and live load of 143 kPa. In the process of consolidation settlement, the surcharge load became less due to buoyancy effect when part of surcharge fill began to submerge as a result of settlement. To avoid continuous topping-up of surcharge fill to recover the decreased load, additional surcharge fill was placed in advance. Thus, the surcharge was filled up to approximately +17 m CD, which provided 225 kPa of surcharge load in the initial stage, decreasing to 180 kPa at the end of the consolidation period.

**4.2 Design of soil improvement**

The clayey fill materials in the reclamation area consisted mainly of dredged clayey soil and excavated soil from land construction, which were mostly compressible. Thus, soil improvement was required to ensure that residual settlement during the in-service

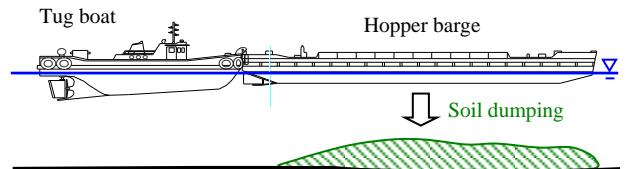


Figure 7 Reclamation method of clayey soil by use of barge



Photo 2 Hopper barge and soil-dumping operation



Photo 3 Reclamation of sand fill and PVD installation

period of the terminal would be within the acceptance criteria.

The method of soil improvement was based on the acceleration of the consolidation process by shortening the drainage path and temporarily increasing the overburden pressure. In this method, the excess pore pressure in clayey soils due to overburden pressure of self-weight and surcharge was dissipated. Otherwise, the dissipation process would take a long time to complete in the natural process because of inherent low permeability of clayey soils.

To reduce the drainage path and expedite dissipation of excess pore water from low-permeable clayey soils, prefabricated vertical drains (PVD) were installed throughout the compressible layer. These drains effectively shorten the drainage path within the clayey layer, and pore water dissipates radially to the nearest drain. Excess water then flows upwards within the PVD and eventually flows out to the sandy fill layers, thus expediting the consolidation process. By shortening the period of soil improvement through the use of PVD and by imposing a surcharge load, over-consolidated conditions were generated in the clayey layers. This will reduce residual settlement under live load and secondary consolidation during the in-service period of the terminal.

A schematic diagram of the soil improvement work is shown in Figure 8. The work was initiated with sand fill capping up to +3.5 m CD, and then PVD was installed through the compressible strata into the residual soil with SPT-N > 30. The maximum depth of PVD penetration was -35 m CD from +3.5 m CD. After installation of PVD, sand fill was placed, and surcharge fill exceeding 180 kPa was imposed at +4.5 m CD. As mentioned in the previous section, in order to avoid continuous topping-up of surcharge fill, additional surcharge fill was placed in advance, up to approximately +17 m CD. The removal of surcharge was allowed only after achievement of specified consolidation degree.

As for the design of PVD, the pitch of the PVD was designed to achieve at least 95% of primary consolidation degree at any depth within the period of 180 days, which was planned for the surcharge construction and loading stages. The PVD with cross

section of 100 mm wide and 5 mm thick, as shown in Photo 4, was installed in square grid pattern, with a spacing ranging from 0.9 to 1.5 m depending on the ground condition based on the analysis of Barron's theory. The total length of PVD used in this project was 23,000 km.

In the analysis of consolidation settlement, residual settlements in the sand, residual soil with SPT-N greater than 30 and rock were not considered due to the high stiffness of these soils. Hence, PVD was installed through the clay fill to the top of residual soil of clay with SPT-N > 30 or rock.

The dredged clayey soil consisted of approximately 20% marine clay and 80% residual soils. The main reclamation area was divided into 10 zones of soil improvement. Numerous consolidation tests were conducted to understand the soils' compressibility and determine the design parameters. Due to variability of the soils, compressibility properties were proposed for each zone of the improved area. The ranges of consolidation parameters are summarized in Table 3.

The estimated range of settlement was 0.8 to 2.3 m, which was consistent to the recorded settlement.

The rebound and settlement upon removal of the surcharge was observed. The rebound observation and assessment are crucial for validating the specified residual settlement of 300 mm under port loading during 50 years after the completion of reclamation work.

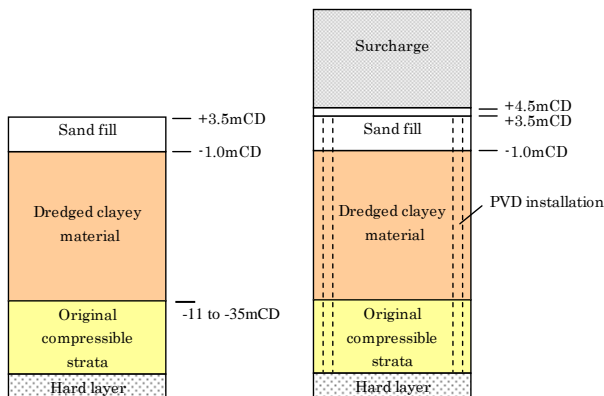
Figure 9 shows a typical soil layer model considering reclamation for a deep-water zone (Zone A) located farthest offshore as shown in Figure 5 and Figure 16. In this zone, the



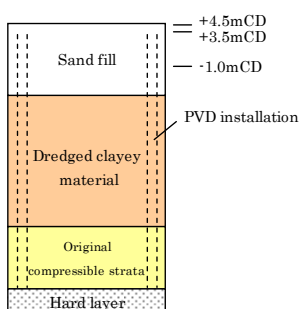
Photo 4 Installed prefabricated vertical drain

Table 3 Consolidation properties of clayey fill

Soil type	Dredged and excavated clay
Wet density ( $Mg/m^3$ )	1.73- 1.85
Natural void ratio	0.90- 1.05
Compression index $c_c$	0.5- 0.6
Recompression index $c_r$	0.025 - 0.045
Preconsolidation pressure $p_c$ (kPa)	80 - 230
Coefficient of consolidation $c_v$ ( $m^2/year$ )	3 - 6



(1) Before PVD installation (2) After PVD installation and surcharging



(3) After consolidation process and surcharge removal

Figure 8 Schematic diagram of soil improvement work

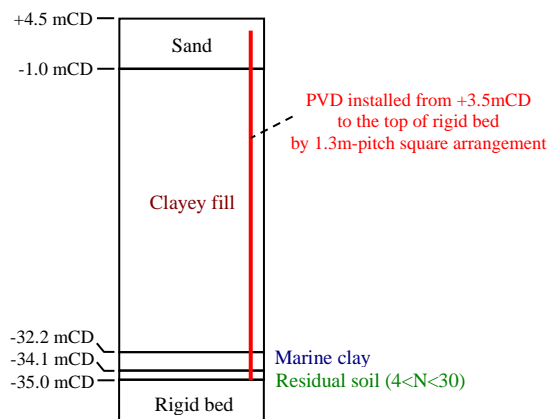


Figure 9 Soil layer model at Zone A in deepwater

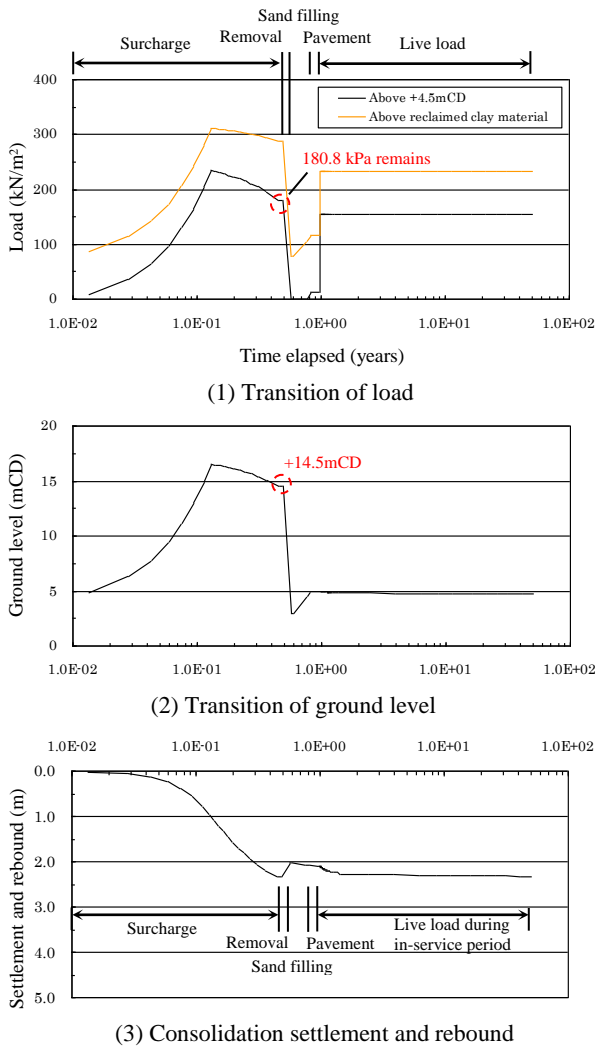


Figure 10 Results of analysis during the stages in the soil improvement by consolidation in Zone A

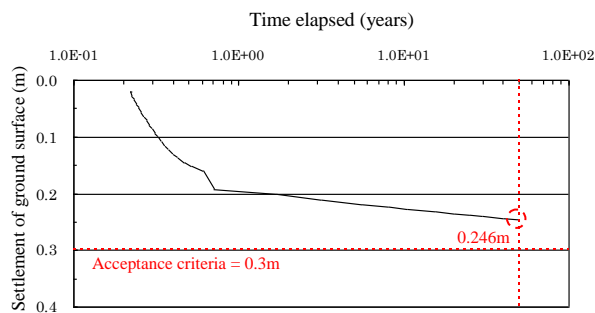


Figure 11 Predicted progress of settlement after the completion of reclamation work in Zone A

reclamation fill was relatively thick at 30 m, and significant large consolidation settlement was predicted during and after soil improvement.

Figure 10 shows a result of design calculation on consolidation settlement during surcharging, surcharge removal and secondary consolidation stage based on the  $c_c$  method and Barron's theory. The settlement after the reclamation work, which includes the effects of secondary consolidation, during the specified 50-year period of port usage was estimated as shown in Figure 11. At this point, coefficient of secondary compression  $c_\alpha$  was set at  $0.04 \cdot c_c$  with reference to recompression index  $c_r$  since the clayey soil was expected to be sufficiently overconsolidated against the magnitude of the future live load.

Based on the prediction, the final residual settlement was 0.246 m, which was within the acceptance criteria of 0.300 m.

### 4.3 Effects of soil improvement

The soil improvement by accelerating consolidation was carried out for soft clayey layer such as clayey fill, the marine clay, the residual soil with SPT-N less than 30, etc. by imposition of surcharge load and installation of PVD. The progress of consolidation was monitored by the settlement plates placed on the level of +3.5 m CD as soon as the installation of PVD was completed.

Figure 12 shows a typical site record of the progress of surcharge height and consolidation settlement in Zone A described in the previous section. The expected final settlement ( $U = 100\%$ ) was interpreted by use of the hyperbolic method (ex. Tan *et al.*, 1991), and the initialization point of the analysis, at which the surcharge load ceased increasing, is also shown in this figure. Figure 13 shows the analysis by the hyperbolic method based on the recorded settlement data in Figure 12. In the procedure of analysis, the adjusted settlement  $S(\text{adj})$  and adjusted time  $t(\text{adj})$  were preparatorily obtained by taking the difference between the observed values and the reference values at the initialization point. Then, the relationship between  $t(\text{adj})$  and  $t(\text{adj})/S(\text{adj})$  was examined on the basis of the theory of the hyperbolic method. The gradient of the linear line plot was 3.02. Considering the settlement at the initialization point  $S_0$  of 1.63 m, the final settlement was estimated at 1.96 m. As the last recorded settlement was 1.87 m, calculation (of the ratio of recorded settlement to final settlement) yielded a degree of consolidation of 95.3% at that point in time, which was more than the 95% specified degree of consolidation. The period of surcharge construction and loading was approximately 170 days.

After the specified degree of consolidation was achieved, the surcharge fill was removed, completing the soil improvement. Then, selected laboratory and in-situ tests were carried out to verify the effectiveness of soil improvement work. For the laboratory tests, piston thin-wall samplers, which are suitable for soft cohesive soils, were used to obtain undisturbed soil samples.

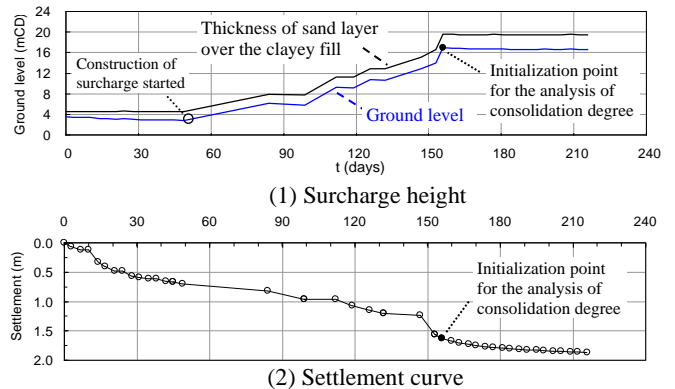
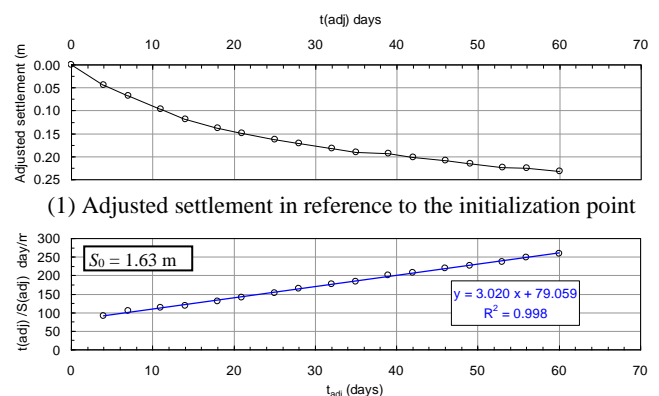


Figure 12 Example of progress of surcharge height and consolidation settlement in Zone A



(2)  $t(\text{adj})$  versus  $t(\text{adj})/S(\text{adj})$  plot

Figure 13 Analysis by the hyperbolic method

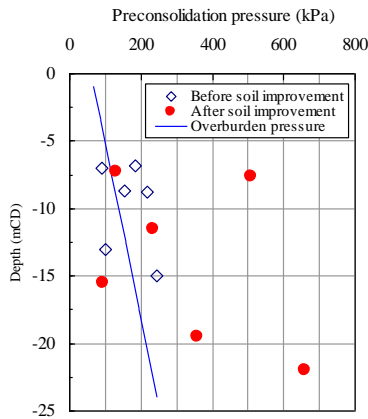


Figure 14 Comparison of preconsolidation pressure before and after soil improvement in Zone A

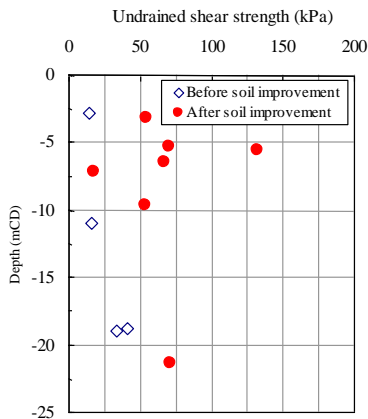


Figure 15 Comparison of undrained shear strength before and after soil improvement in Zone A

Figure 14 shows the preconsolidation pressures obtained from consolidation tests prior to and after soil improvement. It was noted that the average preconsolidation pressure after the soil improvement was 331.5 kPa, compared to 166.0 kPa before the improvement although variation of data is recognized. The variation or low values of test data might be caused by some disturbance in soil sampling work. However, considering the future load of 155 kPa, the effectiveness of soil improvement is confirmed with sufficient increase of the pressure.

Besides the compressibility parameters, some tests were carried out to determine the improved shear strength. Figure 15 shows undrained shear strengths obtained by TX-UU Test. The average improved shear strength was increased from 26.5 kPa to 66.7 kPa. It is expected that closure of the gaps or voids between the clay-fill lumps (created during the process of soil dumping) and micro voids, during the soil improvement process contributes to the shear strength increment.

The soil improvement performance was satisfactorily verified by the desirable results of the in-situ and laboratory tests.

## 5 CONTAINMENT BUND

### 5.1 Design of containment bund

In the process of reclamation by dumping of clayey soil from a hopper barge, the spreading of turbidity of seawater to the surrounding area was a concern. Hence, a containment bund was planned to be placed in advance of reclamation work to create a containment area along with caisson quay walls. The bund was intended to prevent the turbidity from spreading to the nearby natural environment during the reclamation work. In addition, the bund was expected to function as a temporary earth-retaining structure to retain clayey and sandy fills during the progress of reclamation.

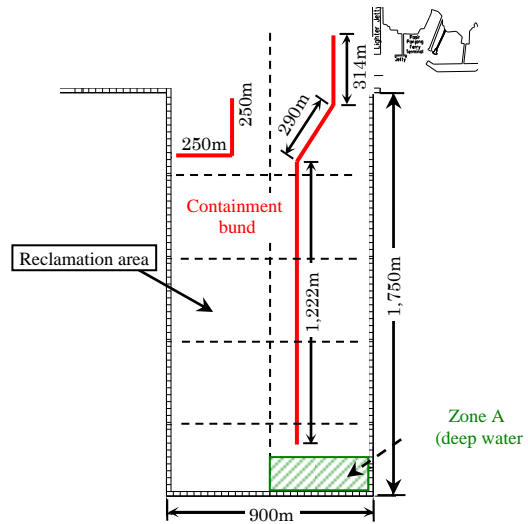


Figure 16 Layout of containment bund

Figure 16 shows the layout of the bund, indicated by red lines. The main bund was positioned to divide the whole area in the cross-shore direction. The initial reclamation filling work commenced from the existing shoreline and proceeded on the left (west) side of the main containment bund.

As described in Section 3 and Figure 6, the core body of the bund consisted of cement-mixed soil (CMS), which was produced from dredged and excavated clayey soils mixed with cement. Prior to CMS filling as core of the bund, geotextile tubes were installed at both sides in order to retain CMS slurry that was filled in between the tubes. The geotextile tubes were also filled with CMS.

#### 5.1.1 Cement-mixed soil (CMS)

The cement-mixed soil has the great advantage that it can be placed even in narrow spaces by pumping injection at the filling stage, and it changes to stiff soil with time by the solidifying effect of cement. The strength can be desirably controlled by adjusting cement content. Application of cement-mixed soil and designing for optimal strength are described by Akimoto *et al.* (2014). That paper described CMS placed to confine polluted mud that had accumulated within a port.

In the construction of Pasir Panjang Terminal Phases 3 and 4, the unconfined compression strength of the CMS was carefully designed such that it fulfilled the stability of the containment bund during reclamation work, preventing the occurrence of global slip failure, and at the same time, the strength was weak enough not to impede future piling work. With those considerations, the design unconfined compression strength,  $q_{u(d)}$ , was set at 200 kPa, which was converted to SPT-N value of 16 by using the formula of Terzaghi and Peck (1948) shown in the following equation.

$$q_u = 12.5N \quad (1)$$

where  $q_u$  is unconfined compression strength (kPa), and N denotes SPT-N value.

To allow for variability of strength, a higher in situ average unconfined compression strength,  $q_{u(f)}$ , was set at 260 kPa by multiplying the design strength by a factor of 1.3 according to the performances in the previous applications in Japan, referring to Coastal Development Institute of Technology, Japan (2008). The applied factor of 1.3 is equivalent to a coefficient of variance of less than 35%, assuming a normal distribution. The deficiency ratio below the design strength was less than 25% of the allowable design shear stress as illustrated in Figure 17.

In order to determine the optimal mix proportion of water and cement for producing the CMS, mix proportion tests were carried out in a laboratory. In the laboratory tests, the mixture of soil

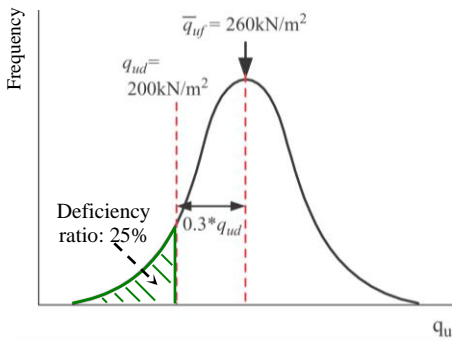


Figure 17 Illustration of design and field strengths of CMS

with cement slurry was carried out by use of mechanically-rotating blades so that uniform and ideal mixing conditions could be achieved.

The target strength in the laboratory of  $q_{u(l)}$  was set at 371 kPa based on the strength ratio  $\beta$ , defined as the ratio of strength of CMS cast underwater in-situ to that produced in the laboratory, of 0.7. This value was derived on the basis of performance in past projects in Japan (Coastal Development Institute of Technology, Japan, 2008). The target strength of 371 kPa was determined to achieve the average strength in-situ of 260 kPa.

Considering the target laboratory strength of 371 kPa and suitable fluidity with the flow value of 140 mm in a table flow test for the clay soil before the addition of cement, the optimal cement dosage was determined to be 60 to 80 kg/m<sup>3</sup> supposing the water/cement ratio is 1:1. The flow test was carried out by placing the soil sample inside an acrylic cylindrical container (8 cm diameter and 8 cm height), and by measuring the diameter of the spread after carefully lifting up and removing the container.

The shear behavior and strength characteristics of CMS were examined by various triaxial shear tests such as unconsolidated undrained triaxial compression test (UU test), consolidated undrained triaxial compression test with pore-water pressure measurement (CIU test), and consolidated drained test (CD test). The CIU and CD tests were carried out under compression unloading state in accordance with the active earth pressure condition, as shown in Figure 18, in addition to the standard compression loading tests. The behavior in post-peak strength state was also investigated. Marine clay with high liquid limit and the residual soil with lower liquid limit were chosen to produce the CMS. The water content before addition of cement was approximately 180% in the case of marine clay and 110% in the case of residual soil.

Figure 19 shows the results of compression CIU test. It shows strain softening behavior after the peak stress, which occurred at about 1.5% strain. The residual strength ratio is defined as the ratio of the residual strength at the axial strain of 10-15% to the peak strength. It was apparent that the residual strength ratio of 0.6 to 0.9 in residual soil samples with low water

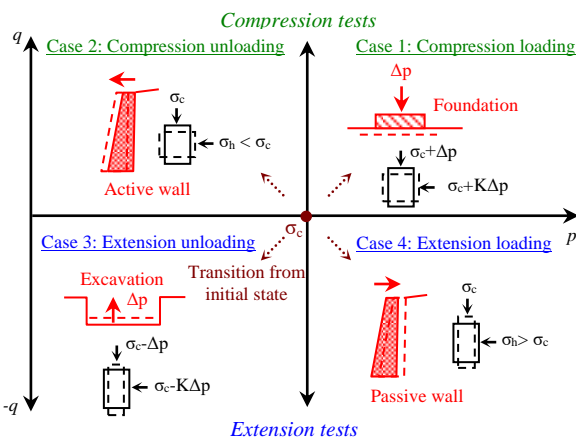
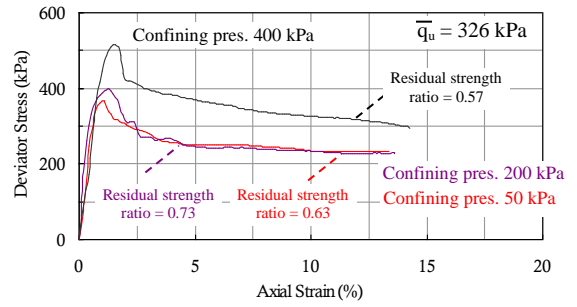
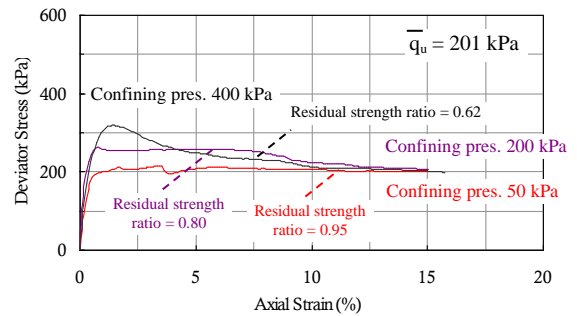


Figure 18 Loading states in p-q stress plane



(1) Base soil: Marine clay



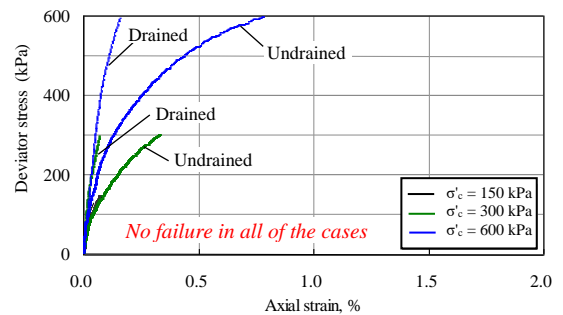
(2) Base soil: Residual soil

Figure 19 Stress-strain curve in CIU tests

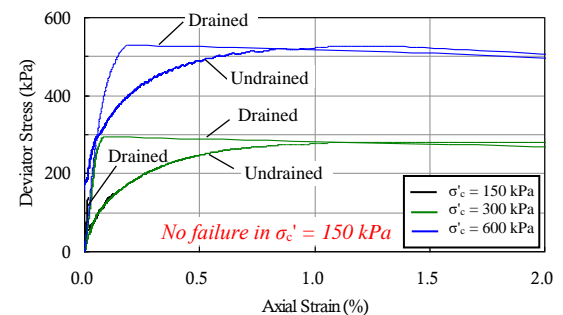
content was higher than that of 0.5 to 0.7 in marine clay samples with high water content. It was concluded that the residual strength ratio was affected predominantly by water content of the soil slurry.

Figure 20 shows the stress-strain curve obtained from CIU and CD tests in the compression loading conditions. The tests were conducted by decreasing cell pressure while the axial pressure is maintained constant. In the tests, no failure took place in the case of marine clay sample even when the confining pressure was decreased to zero. On the contrary, the failure took place in residual soil sample after the stress reached the maximum obtained from the standard CIU tests. Similar behavior was observed for residual soil sample under CD test.

All of the results of CIU and CD tests for cement-mixed soils

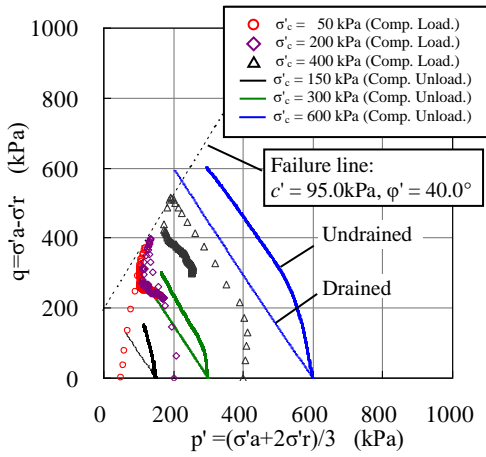


(1) Base soil: Marine clay

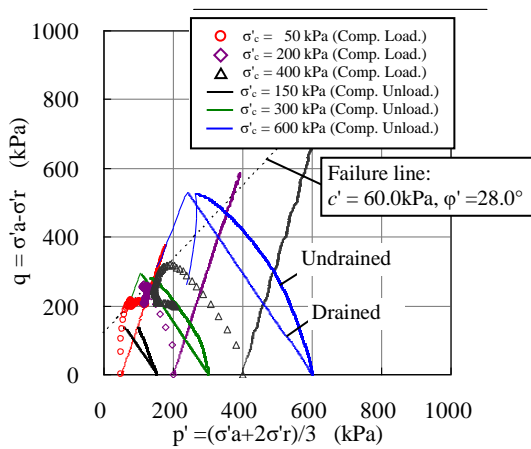


(2) Base soil: Residual soil

Figure 20 Stress-strain curve in the compression unloading condition (active earth pressure condition)

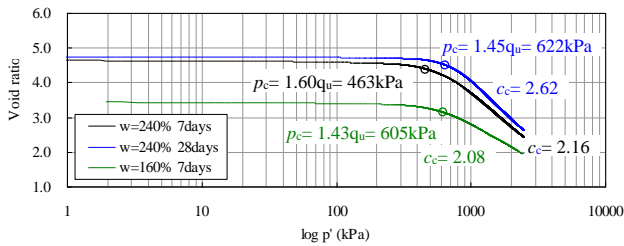


(1) Base material: Marine clay

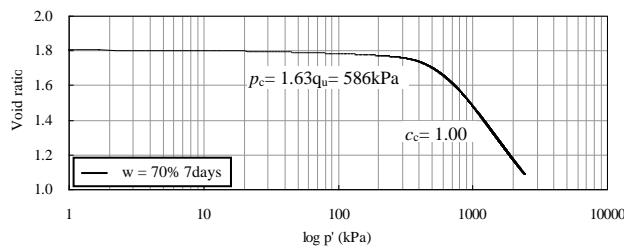


(2) Base material: Residual soil

Figure 21 Effective stress paths of the CMS obtained by CIU and CD tests



(1) Base soil: Marine clay



(2) Base soil: Residual soil

Figure 22 Relationship between  $e$  and  $\log p'$  obtained by constant strain rate consolidation test

are presented in  $p'$ - $q$  effective stress plane and are shown in Figure 21. From the figure, it can be deduced that failure occurred along the unique line obtained by CIU tests in the standard loading conditions. Hence for the design, the proposed effective residual strength for CMS was cohesion  $c'_r$  of 0 and effective angle of shearing resistance  $\phi'_r$  of  $30^\circ$ , while the peak strength cohesion  $c'$  of 40 kPa and effective angle of shearing

Table 4 Proposed consolidation parameters of CMS used in design

Compression index $c_c$	2.3
Recompression index $c_r$	$0.006(1+e_0)$
Preconsolidation pressure $p_c$ (kPa)	$1.5q_u = 390$ kPa
Coefficient of consolidation $c_v$ ( $m^2/year$ )	150

resistance  $\phi'$  of  $40^\circ$ . For reference, the properties on shear strength of original marine clay are given as  $c' = 20$  kPa and  $\phi' = 24^\circ$ , and those of original residual soil are given as  $c' = 0$  kPa and  $\phi' = 25$  to  $35^\circ$ .

The recommended saturated unit weight of CMS is  $14 \text{ kN/m}^3$ .

To obtain the consolidation properties of CMS, constant strain rate consolidation tests were carried out. Figure 22 shows the relationship between void ratio and consolidation pressure that were obtained by the consolidation tests. It is shown clearly that the preconsolidation pressure was related to the unconfined compression strength. It is also interesting to note that a significant drop in void ratio was recorded once consolidation pressure exceeded the preconsolidation pressure. The compression index in highly compressible marine clay sample was nearly 1.0. The increase of compressibility of CMS at normal consolidation state was attributed to the increase of voids in the soil skeleton by adding water in the production of CMS. The proposed design parameters for consolidation analysis are summarized in Table 4.

### 5.1.2 Containment bund

In conventional applications, large-scale soil bags with volume of tens to hundreds of cubic meters have been applied as a jetty, submerged breakwater, coastal embankment, etc. for coastal protection as reported by Heerten *et al.* (2000) and McClarty *et al.* (2006).

In this project, cement-mixed soil was used in a challenging new way; to construct a submerged temporary earth retaining structure.

The containment bund was constructed by placing of geotextile tubes filled with CMS at the sloping sides and infilling between the geotextile tubes with CMS. Figure 23 shows the cross-section of the bund.

For large-scale placing of soil bags underwater, two methods are generally applied as shown in Figure 24 and Figure 25. These methods were introduced by Pilarczyk (2000). One method is releasing a soil bag from a split hopper barge after filling of the bag inside the barge's hopper. The other is filling the soil bag that has been laid on the bed in advance.

In this project, both methods were adopted to place the geotextile tubes. The tubes were equipped with injection and drainage ports. In the first method, CMS slurry was filled into the tube through the injection port while the tube was in the barge's hopper. After completing the filling, the geotextile tube was released from the barge to its final position.

The dimensions of the geotextile tubes were 27 m in length and 19.5 m in perimeter, with a full capacity of  $800 \text{ m}^3$ . The tube was filled to 70% capacity, which meant  $560 \text{ m}^3$  of CMS was filled in each tube.

The shape of the geotextile tube with infill material was

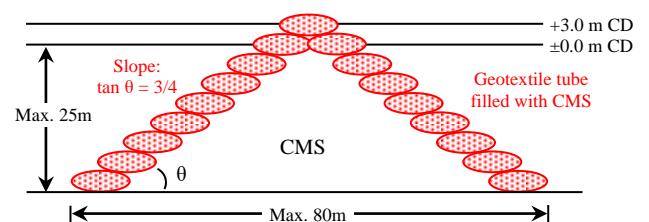


Figure 23 Cross-sectional view of containment bund

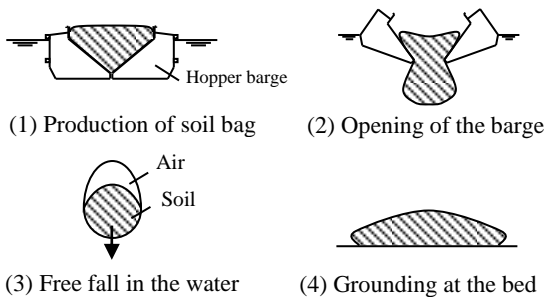


Figure 24 Placement of soil bag by dumping

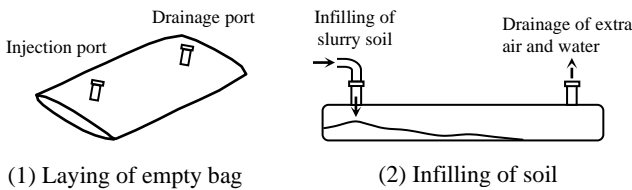


Figure 25 Placement of soil bag by infilling soil into laid bag

analyzed by use of the method proposed by Leshchinsky *et al.* (1996), solving the following non-linear second-order differential equation with boundary conditions in the  $x, y$  coordinates shown in Figure 26.

$$T \frac{d^2 y}{dx^2} - (p_0 + \gamma x) \cdot \left[ 1 + (dy/dx)^2 \right]^{3/2} = 0 \quad (2)$$

$$y|_{x=0} = 0 \quad y|_{x=h} = \frac{\gamma}{p_0 + \gamma h} \int_0^h y(x) dx \quad (3)$$

$$\frac{1}{(dy/dx)|_{y=0}} = 0 \quad (4)$$

$$S = \frac{2\gamma}{p_0 + \gamma h} \int_0^h y(x) dx + 2 \int_0^h \left[ 1 + \left( \frac{dy}{dx} \right)^2 \right]^{1/2} dx \quad (5)$$

where  $S$  is perimeter,  $\gamma$  is unit weight of fill material,  $p_0$  is pumping pressure and  $T$  is tensile force to geotextile.

The analyzed shape of the tube is shown in Figure 27. The filled tube was approximately 3 m high and 8 m wide. The induced tensile force in the geotextile was calculated to be 39 kN/m in the onshore condition, meaning that this force arises at the infill production stage. In order to determine the tensile strength of geotextile, factors of safety for installation damage, pumping pressure fluctuation and seam strength were considered. Adopting a total safety factor of 3.0, the required design strength at the production stage  $T_{d(p)}$  was determined as  $T_{d(p)} = 39.0 \times 3.0$

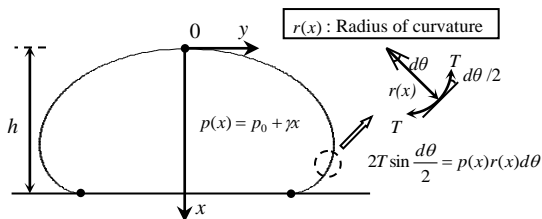


Figure 26  $x$ - $y$  coordinate in the shape analysis of geotextile tube

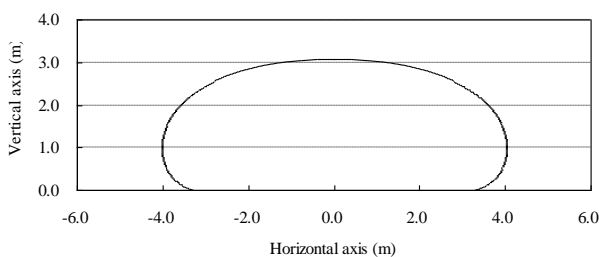


Figure 27 Analyzed shape of geotextile tube

= 120 kN/m.

In the case of placement by dumping shown in Figure 24, significant forces occur at the stages of the opening of the barge, the free-fall in the water, and the impact grounding at the seabed, as described by Pilarczyk (2000).

In the stage of the opening of the barge, the soil bag is held by the friction between the bag and the barge for a while. At this time, the weight of bag is balanced with the tensile force to the geotextile. The tensile force was evaluated by use of the following formula proposed by Bezuijen *et al.* (2004).

$$T = 0.45W'/L \quad (6)$$

where  $T$  is tensile force to the geotextile,  $W'$  is weight of soil bag in the water, and  $L$  is length of the bag in the longitudinal direction.

In the stage of free fall in the water, buoyancy effect appears by the presence of air entrapped inside the bag. The upward force due to buoyancy should be balanced with tensile forces to the geotextile, and the tensile force is evaluated by the following formula proposed by Bezuijen *et al.* (2000).

$$T = 0.5(1 - R_f)H'B'(\gamma_w - \gamma_{air}) \quad (7)$$

where  $R_f$  is filling rate of soil in the bag,  $H'$  and  $B'$  are the height and width of soil bag in the hopper of a barge respectively,  $\gamma_w$  and  $\gamma_{air}$  are unit weight of sea water and air respectively.

Upon grounding at the seabed, the kinetic energy of the soil bag with significant fall velocity is converted to elastic energy of geotextile, which is generated by tensile force. Referring to Bezuijen *et al.* (2000), the tensile force to the geotextile at this stage is evaluated by solving the following equation.

$$\frac{1}{2} \rho A v_b^2 = \frac{1}{2} \frac{S}{E'} T^2 + P f_r b^2 \quad (8)$$

where  $\rho$  is density of fill material,  $v_b$  is falling velocity at the grounding,  $A$  is cross-sectional area of the bag,  $E'$  is stiffness modulus of geotextile,  $P$  is pressure on the bottom during the impact,  $f_r$  is friction coefficient between the geotextile and the subsoil,  $b$  is half of the length of the soil bag that touches the subsoil upon the impact.

In the above equation, the term in the left-hand side means kinetic energy of the soil bag, while in the right-hand side, the first term means the elastic energy in the geotextile and the second term means the friction between the geotextile and the subsoil.

The tensile forces at the above stages were evaluated as 42 kN/m at the opening of the barge, 66 kN/m at the free fall

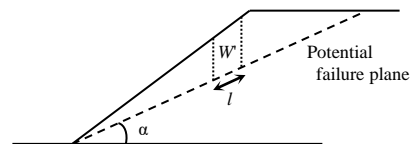


Figure 28 Assumed slip failure plane geometry at bund

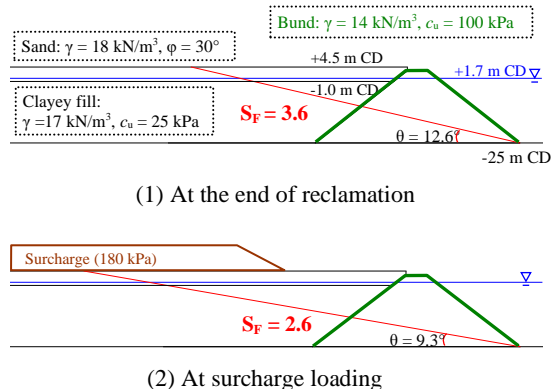


Figure 29 Safety factor for the stability against slip failure 40

in the water and 171 kN/m at the impact grounding. In particular, the force at the impact grounding depends on water depth. In the design calculation, the water depth was conservatively set at 25 m, which was the maximum depth in the site. Considering the predicted tensile forces at the production and placement stages, the design tensile strength of the geotextile was set at 180 kN/m.

The stability of the containment bund was examined at the stages of completion of reclamation and imposition of surcharge load. A straight line was assumed as the potential failure surface as shown in Figure 28. The failure plane does not extend beyond the base of the CMS since the containment bund was planned to be constructed on the rigid layers of the residual soil with SPT-N value greater than 30.

The safety factor against slip failure is expressed by the following formula.

$$S_F = \frac{\sum [cl + (W' \cos \alpha) \tan \phi]}{\sin \alpha \sum W'} \quad (9)$$

where  $S_F$  is safety factor,  $c$  is cohesion of soil,  $\phi$  is angle of shear resistance,  $l$  is length fragment at the bottom,  $W'$  is weight of fragment, and  $\alpha$  is angle of potential failure plane.

The calculated safety factors are shown in Figure 29. The containment bund was considered stable as the safety factor against slip failure was greater than 1.5 at both completion of reclamation and during surcharge loading.

**5.2 Construction of containment bund**

In the construction sequence of the containment bund, firstly CMS-filled geotextile tubes were placed on the seabed along the designated sides of the bund. Then, CMS slurry was filled into the space bounded by the tubes up to the top level of the tubes. After solidification of the CMS, the second layer of CMS-filled geotextile tubes was placed on the flat top, followed by filling of CMS slurry in the bounded space. By repeating these procedures, the containment bund with steep side slopes of 1:1.33 ( $\tan \theta = 0.75$ ) was constructed.

**5.2.1 Production of CMS**

The base soils of dredged clay, which consisted of mainly of residual soil, and excavated clay from onshore construction were too stiff and hard for homogeneous mixing with cement and pumping injection in the construction work of CMS. Hence, as advanced preparation, these soils were broken down and softened to a slurry state with addition of water prior to the production of CMS.

The production sequence of CMS was as follows.

(1) Dredged and excavated soils were transported by a barge to the construction area, and they were transferred to a working barge by backhoes on a transfer barge as shown in Photo 5.

(2) The soil was broken down and softened to slurry state with addition of water by use of grippers and backhoes with special mixing buckets. The volume of water to be added was determined so that the designated flow value of 140 mm  $\pm$  10 mm in the table flow test could be realized. Breaking and mixing of base soil are shown in Photo 6.

(3) The barge with slurry soils was brought alongside the CMS production and pumping barge. The soils were brought sequentially to the feeding hopper of the production barge, and inside the vessel, cement was added to the soil and mixed together.

(4) After producing the CMS in the vessel, the CMS in slurry state was transported and cast to the target position underwater through a tremie pipe by pump pressure as shown in Photo 7.

The quality of CMS was examined by unconfined compression tests on the specimens, which were sampled at the point of production in the vessel and cured in a laboratory for

28 days. This strength was compared with the target strength in the laboratory  $q_{u(l)}$  of 371 kPa. That is, it was considered that



Photo 5 Transferring soil



(1) Breaking (2) Mixing

Photo 6 Soil breaking and mixing

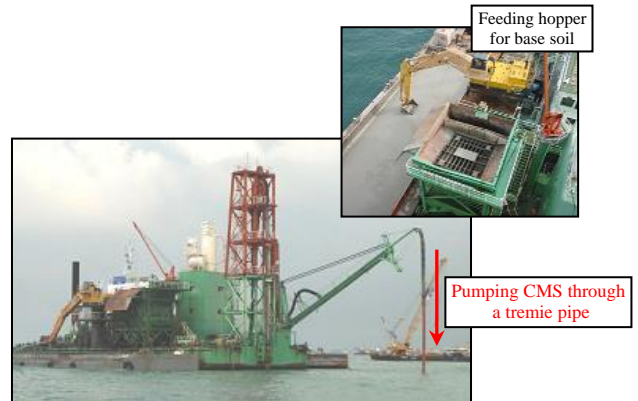


Photo 7 Pumping of CMS from the production barge

the quality of the CMS cast underwater was satisfactory in the condition that the strength of specimen exceeds the target strength in a laboratory.

Figure 30 shows the results of unconfined compression tests on the specimen produced in the vessel that experienced 28 curing days. The average strength was 448 kPa, which was larger than the target strength by 20%. As for the variability of strength, the coefficient of variation was 37%, which was comparable to the expected level of 35% in the design. The quality of CMS placed underwater in situ was judged as satisfactory based on the results of average strength and the coefficient of variation on the specimen.

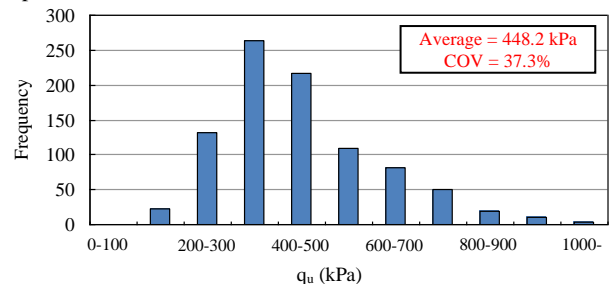


Figure 30 Strength of CMS specimens produced on the barge



Photo 8 Condition during CMS filling and after dumping

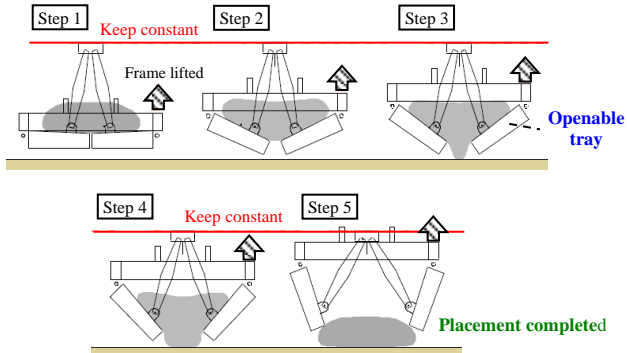


Figure 31 New placement method by use of openable tray with rise and fall system

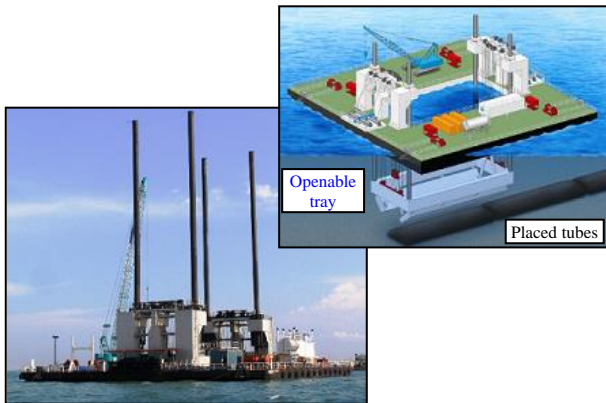


Photo 9 Special vessel for placing geotextile tubes

### 5.2.2 Placement of geotextile tubes

The geotextile tubes were constructed and placed by use of a hopper barge. Firstly, the slurry CMS, which was produced in the production barge, was injected into empty geotextile tubes in the hopper of the barge, and after filling the tube with CMS, it was dumped from the barge through the bottom opening. The condition in the hopper during CMS filling and after dumping is shown in Photo 8.

In the accumulation of results of the dumping placement, it turned out that a significant proportion of tubes burst at the grounding impact. Hence, for stable placement, dumping was delayed for approximately 3 to 4 hours to allow stiffening of the CMS due to hydration of the cement. In addition, it was considered that the precision of the dumped position compared to the design position should be improved. Especially in deeper area, the deviation tended to be significant.

Facing these difficulties, a new special vessel was built exclusively in order to place geotextile tubes stably in the exact positions. The concept of the new installation method is illustrated in Figure 31. In this method, a geotextile tube was

produced on the openable tray, which has a rise and fall system. When placing the tube, the tray was lowered toward the



(1) Laying of empty tube (2) Filling CMS into tube



(3) Filling completed

Photo 10 Production of geotextile tube in the special vessel



Photo 11 Containment bund completed by geotextile tubes and infill of CMS



Photo 12 Completed reclamation of Pasir Panjang Terminal Phases 3 and 4

placement depth. At a height of 50 cm above the bottom, the tray was opened, and while keeping the height constant, the geotextile tube was placed softly at the target position.

Photo 9 shows the newly-built vessel, and the production of a geotextile tube in the vessel is shown in Photo 10. By introducing the new vessel, nearly 90% of geotextile tubes were successfully placed at the target positions without bursting against severe conditions of maximum 25 m of water depth and maximum 1.3 m/s of tidal current.

The crest of the containment bund, successfully completed by geotextile tubes and infill of CMS, is shown in Photo 11.

## 6. CONCLUSION

In the large-scale reclamation of Pasir Panjang Terminal Phases 3 and 4, innovative geotechnical solutions were implemented by reusing and recycling clayey soils from dredging of fairways and basins and excavated soil from onshore sources. In this project, 50 million cubic meters of reclamation fill was required, and nearly half of it was clayey soil as alternative material.

Overcoming challenges in the soil improvement by accelerating consolidation with installation of PVD and imposition of surcharge and in the construction of the innovative containment bunds, the land reclamation for Pasir Panjang Terminal Phases 3 and 4 was successfully completed as shown in Photo 12. Pasir Panjang Terminal Phases 3 and 4 will strengthen the position of Singapore as the world's largest transshipment hub.

The problems of shortage of good sandy soil and difficulty of disposal of unwanted clayey soil are not limited to Singapore, but are encountered globally. On the other hand, the disposal of unwanted soils, which come from excavation in land construction or dredging in marine construction or port maintenance, etc., is a serious problem because the construction of disposal sites has significant economic and environmental impacts. The methods of reusing and recycling clayey soils presented in this paper can help to resolve these problems, contributing to realization of sustainable development in the world.

## 7. REFERENCES

- Akimoto T., H. Shinsha, T. Kumagai, and T. Horiuchi (2014): Execution method of cement mixed soils for confining fluid mud, 7th International Congress on Environmental Geotechnics, Engineers Australia, pp. 520-526.
- Bezuijzen A, Adel, H. den, Groot M. B. and Pilarczyk K. W. (2000): Research on geocontainers and its application in practice, Proc. 27th ICCE., pp. 2331-2341.
- Bezuijzen A., Groot M. B. de, Breteler M. K. and Berendes E. (2004): Placing accuracy and stability of geocontainers, Proc. of the Third European Geosynthetics Conference, Munich, Germany, pp. 123-128.
- Coastal Development Institute of Technology, Japan (2008): The Pneumatic Flow Mixing Method Technical Manual, 188 p. (in Japanese)
- Heerten G, A. Jackson, S. Restall and F. Saathoff (2000): New Geotextile Developments with Mechanically-Bonded Nonwoven Sand Containers as Coastal Structures, Proc. 27th ICCE, pp. 2342-2355.
- Kitazume M. (2017): The Pneumatic Flow Mixing Method, CRC Press/Balkema, 233 p.
- Lawson C. (2006): Geotextile containment for hydraulic and environmental engineering. The 8<sup>th</sup> International Conference on Geosynthetics, Yokohama, Japan, pp. 9-48.
- Leshchinsky D., O. Leshchinsky, H. I. Ling and P. A. Gilbert (1996): Geosynthetic tube for confining pressurized slurry, J. of Geotechnical Eng., pp. 682-690, ASCE.
- McClarty A, J. Cross, G. M. James and L. Gilbert (2006): Design and construction of coastal erosion protection groyne using geocontainers, Langebaan, South Africa, Geosynthetics, J. Kuwano and J. Koseki (eds), Millpress, Rotterdam, ISBN 90 5966 044 7, pp. 765-768.
- Pilarczyk K. W. (2000): Geosynthetics and Geosystems in Hydraulic and Coastal Engineering, Balkema, Rotterdam, 913 p.
- Singapore Public Works Department (1976): Geology of the Republic of Singapore. Public Works Department (Singapore).
- Tan T. S., T. Inoue and S. L. Lee (1991): Hyperbolic method for consolidation analysis, J. of Geotechnical Engineering, Vol. 117, No. 11, pp. 1723-1737.
- Terzaghi K. and R. B. Peck (1948): Soil Mechanics in Engineering Practice, John Wiley & Sons, 566 p.